ORIGINAL ARTICLE
RESPIRATORY INFECTIONS

Multiple inflammasomes may regulate the interleukin-1-driven inflammation in protracted bacterial bronchitis

Alice C-H. Chen[1,12], Hai B. Tran[2,12], Yang Xi[1], Stephanie T. Yerkovich[3], Katherine J. Baines[4], Susan J. Pizzutto[5], Melanie Carroll[1], Avril A.B. Robertson[6], Matthew A. Cooper[6], Kate Schroder[6], Jodie L. Simpson[4], Peter G. Gibson[4], Greg Hodge[2,7], Ian B. Masters[8], Helen M. Buntain[9], Helen L. Petsky[10], Samantha J. Prime[11], Anne B. Chang[5,11], Sandra Hodge[2,7,13] and John W. Upham[1,13]

Affiliations: [1]Diamantina Institute, Faculty of Medicine, The University of Queensland, Brisbane, Australia. [2]Dept of Thoracic Medicine, Royal Adelaide Hospital, Adelaide, Australia. [3]The Prince Charles Hospital, Brisbane, Australia. [4]The University of Newcastle, Newcastle, Australia. [5]Child Health Division, Menzies School of Health Research, Charles Darwin Hospital, Darwin, Australia. [6]Institute for Molecular Bioscience, Brisbane, Australia. [7]Dept of Medicine, The University of Adelaide, Adelaide, Australia. [8]Respiratory and Sleep Medicine, Lady Cilento Children's Hospital and Children's Centre for Health Research, Queensland University of Technology, Brisbane, Australia. [9]Wesley Hospital, Brisbane, Australia. [10]School of Nursing and Midwifery, Menzies Health Institute Queensland, Griffith University, Brisbane, Australia. [11]Queensland University of Technology, Brisbane, Australia. [12]Joint first authors. [13]Joint senior authors.

Correspondence: John W. Upham, Translational Research Institute, 37 Kent St, Woolloongabba, QLD 4102, Australia. E-mail: j.upham@uq.edu.au

ABSTRACT Protracted bacterial bronchitis (PBB) in young children is characterised by prolonged wet cough, prominent airway interleukin (IL)-1β expression and infection, often with nontypeable *Haemophilus influenzae* (NTHi). The mechanisms responsible for IL-1-driven inflammation in PBB are poorly understood.

We hypothesised that the inflammation in PBB involves the NLRP3 and/or AIM2 inflammasome/IL-1β axis. Lung macrophages obtained from bronchoalveolar lavage (BAL), peripheral blood mononuclear cells (PBMCs), blood monocytes and monocyte-derived macrophages from patients with PBB and age-matched healthy controls were cultured in control medium or exposed to live NTHi.

In healthy adult PBMCs, $CD14^+$ monocytes contributed to 95% of total IL-1β-producing cells upon NTHi stimulation. Stimulation of PBB PBMCs with NTHi significantly increased *IL-1β* expression ($p<0.001$), but decreased *NLRC4* expression ($p<0.01$). NTHi induced IL-1β secretion in PBMCs from both healthy controls and patients with recurrent PBB. This was inhibited by Z-YVAD-FMK (a caspase-1 selective inhibitor) and by MCC950 (a NLRP3 selective inhibitor). In PBB BAL macrophages inflammasome complexes were visualised as fluorescence specks of NLRP3 or AIM2 colocalised with cleaved caspase-1 and cleaved IL-1β. NTHi stimulation induced formation of specks of cleaved IL-1β, NLRP3 and AIM2 in PBMCs, blood monocytes and monocyte-derived macrophages.

We conclude that both the NLRP3 and AIM2 inflammasomes probably drive the IL-1β-dominated inflammation in PBB.

@ERSpublications
Airway IL-1β activation in protracted bacterial bronchitis http://ow.ly/ut9r30iqim2

Cite this article as: Chen AC-H, Tran HB, Xi Y, *et al.* Multiple inflammasomes may regulate the interleukin-1-driven inflammation in protracted bacterial bronchitis. *ERJ Open Res* 2018; 4: 00130-2017 [https://doi.org/10.1183/23120541.00130-2017].

This article has supplementary material available from openres.ersjournals.com

Introduction

Protracted bacterial bronchitis (PBB) is a pathological entity that is characterised by a chronic wet or productive cough without signs of an alternative cause, and which usually responds to antibiotic therapy [1–4]. The full bacterial spectrum in PBB remains to be specified, but the opportunistic pathogen nontypeable *Haemophilus influenzae* (NTHi) is the most commonly identified organism [1, 5–7], and a risk factor for progression to bronchiectasis [2, 8]. The pathology caused by *H. influenzae* is often due to the pro-inflammatory responses by the host, rather than bacterial "virulence factors" [9].

A limited number of innate immune pathways have been explored in PBB, including pathogen-associated molecular pattern recognition receptors such as Toll-like receptor (TLR)2/4 [10], the collectins mannose-binding lectin and surfactant protein D [11], effector molecules such as matrix metalloproteinase-9, interleukin (IL)-8 [10] and human β-defensin-2 [11]. Although lung cells produce many cytokines in PBB, IL-1β is particularly prominent in the PBB airways compared to healthy airways [12]. Production of IL-1β by monocytes, macrophages and epithelial cells can be stimulated by bacterial infections, including *H. influenzae* [13]. Airway concentrations of IL-1β are strongly associated with symptom severity [14, 15], and we have recently demonstrated that the pro-inflammatory changes in PBB may be associated with defective clearance of NTHi by alveolar macrophages, which poses a risk for development of bronchiectasis [16].

Inflammasomes are intracellular receptors capable of sensing both pathogen-associated and damage-associated molecular patterns (PAMPs and DAMPs, respectively) leading to initiation of a protective inflammatory response *via* activation of potent cytokines of the IL-1 family, *e.g.* IL-1β and IL-18. Inflammasomes are cytosolic multiprotein complexes assembled around a sentinel protein such as NLRP3 (NACHT, LRR and PYD domains-containing protein 3 or NALP3), NLRC4 (NLR family CARD domain-containing protein 4) or AIM2 (absent in melanoma 2), which define the particular type of inflammasome. Upon recognition of a PAMP or a DAMP, the sentinel oligomerises and binds other proteins such as ASC (apoptosis-associated speck-like containing a caspase recruitment domain) and procaspase-1, the latter becoming activated and cleaving/activating precursors of IL-1β/IL-18. Despite numerous studies of IL-1 cytokines and inflammasomes as key mechanisms in initiation and maintenance of chronic inflammation in the lung [17, 18], their role in PBB has been not studied.

Therefore, we investigated the hypotheses that PBB would be associated with assembled inflammasome(s) that activate IL-1 cytokines, and that inflammasome activation could be induced by NTHi. The aims of this study were to examine the role of inflammasomes in NTHi-induced IL-1β production and determine whether NTHi-induced IL-1β production is caspase-1- and NLRP3-dependent.

Methods

Subjects and procedures

This study was approved by the ethics committees of Children's Health Queensland (HREC/03/QRCH/17), Queensland University of Technology (1400000072), Uniting Care Health (1418) and University of Queensland (2008000064 and 2008000037). Informed consent was obtained from each participant's parents/legal guardians. Children in the experimental cohort were recruited prior to undergoing flexible bronchoscopy, for any clinical indication, as arranged by their treating physician. Diagnosis of recurrent PBB was based on a wet cough on the day of bronchoscopy, airway neutrophilia (>15%) and more than three separate PBB episodes within 12 months following bronchoscopy. Diagnosis of bronchiectasis was based on chest computed tomography using established criteria [19]. Children in the control arm were age-matched subjects with no current or previous respiratory conditions. Medical history was obtained for all participants, and parents of children with PBB and bronchiectasis completed a cough diary [20] which was followed-up for 12 months. Blood buffy coat from adults was obtained from the Australian Red Cross Blood Service (mater supply agreement 15-06QLD-06).

Received: Oct 26 2017 | Accepted after revision: Feb 08 2018

Support statement: A.B. Chang and P.G. Gibson are supported by National Health and Medical Research Council (NHMRC) practitioner fellowships (grants 1058213 and 1058552). The study was supported by NHMRC project grant (1042601) and the Centre for Research Excellence (CRE) for Lung Health in Indigenous Children. A.C-H. Chang is supported by postdoctoral fellowships funded by the NHMRC CRE for Lung Health in Indigenous Children (1040830). M.A. Cooper is supported by a NHMRC PRF (1059354). S. Hodge is supported by a University of Adelaide Professorial Research Fellowship. H.L. Petsky is supported by an early career fellowship from Asthma Australia. Funding information for this article has been deposited with the Crossref Funder Registry.

Conflict of interest: None declared.

Bronchoalveolar lavage fluid sample processing and immune cell isolation

Bronchoscopy and bronchoalveolar lavage (BAL) was performed using standardised methods as per European Respiratory Society guidelines [21], and as detailed in our prior publications [11, 22]. The first aliquot was used for microbiological testing and the second and third were pooled for cellularity studies. BAL fluid was centrifuged at 600×*g* for 10 min at 20°C to pellet all nucleated cells. BAL-derived alveolar macrophages were purified as previously described [23]. Briefly, the cell pellet was washed twice before plating out on a 96-well flat-bottomed plate (Costar, Corning, NY, USA) at 50 000 cells·well^{-1} with 10% heat-inactivated (HI)-fetal calf serum (FCS)/penicillin, streptomycin and L-glutamine (PSG)/RPMI (LifeTechnologies, Carlsbad, CA, USA). The cells were incubated at 37°C/5% carbon dioxide (CO_2) for 2 h to allow adherence of macrophages on the plastic plate. Other cells were separated from alveolar macrophages by removal of supernatants and three gentle washes with PBS. The nonadherent cells were transferred to a 96-well U-bottomed plate (In vitro Technologies, Noble Park North, Australia) for culturing.

PBMC isolation

PBMCs were isolated from whole blood using Lymphoprep gradient media (Stemcell Technologies, Vancouver, Canada) and then cryopreserved in liquid nitrogen. Experiments were performed in batches. The frozen cells were rinsed twice in 2% HI-FCS/PSG/RPMI and rested in culture medium at 37°C/5%/CO_2 for 1 h before the experiment. PBMCs were plated in a 96-well U-bottomed plate at 250 000 cells·well^{-1} with 5% HI-FCS/PSG/RPMI for 24 h culture.

Monocytes and monocyte-derived macrophage culture

PBMCs were incubated at 37°C/5% CO_2 overnight to allow adherence of monocytes on the culture plate. The monocytes were then cultured for 6 days in 10% HI-FCS/PSG/RPMI with or without 50 ng·mL^{-1} granulocyte-macrophage colony-stimulating factor to allow differentiation of monocyte-derived macrophages. In relevant experiments, the cells were mounted on superfrost plus slides using cytospin, and further fixed with 2.5% formalin.

Stimulation with NTHi and caspase-1- and NLRP3-selective inhibition

A single clinical isolate of NTHi was used for all experiments and prepared as previously described [24]. Briefly, the NTHi strain was grown for 8 h in brain–heart infusion broth supplemented with NTHi growth factors. Single-use aliquots were stored in 20% HI-FCS at −80°C. Low-dose NTHi stimulation using 0.33 multiplicity of infection (MOI) (0.2×10^6 cfu·mL^{-1}) for 24 h was applied for all experiments using PBMCs; BAL cells were stimulated with NTHi at 1.5 MOI for 24 h. 40 μM caspase-1 inhibitor (Z-YVAD-FMK) (Merck, Kenilworth, NJ, USA) or 10 μM MCC950 was used to pretreat cells for 1 h before stimulation with NTHi in relevant experiments.

Quantitative reverse transcriptase PCR

BAL was centrifuged at 600×*g* for 10 min at 20°C to pellet all mammalian cells. The cell pellet was washed before storing in RNAprotect Cell Reagent (QIAGEN, Hilden, Germany). Frozen BAL cells were washed in PBS, followed by on-column RNA extraction using the ISOLATE II RNA Micro Kit (Bioline, London, UK) and cDNA synthesis using SensiFAST cDNA Synthesis Kit (Bioline). Changes in expression of genes during inflammation or its resolution was measured using reverse transcriptase (RT)-PCR using SensiFAST SYBR No-ROX Kit (Bioline) and LightCycler 480 System (Roche, Basel, Switzerland). The threshold cycle (CT) of β-actin was used for standardisation, ΔΔCT was applied with CT of housekeeper set to one, and the relative gene expression reported. Primer sequences for RT-PCR are listed in online supplementary table S1.

Cytokine quantification using ELISA

IL-1β concentration in cell free culture supernatant was measured using a commercially available ELISA kit (lowest detection limit was 3.9 pg·mL^{-1}) (BD Biosciences, Franklin Lakes, NJ, USA).

Immunofluorescence, confocal microscopy and quantitative immunofluorescence

Cells were prepared onto chamberslides (macrophages and monocytes) and cytospins (PBMCs), and immunofluorescence-stained as previously described [25]. The primary antibodies from Santa Cruz (Dallas, TX, USA) included goat anticleaved caspase-1 and goat anticleaved IL-1β, the specificity of which was validated by immunogen peptide inhibition [26], rabbit anti-NLRP3, which has been used extensively in previous publications including ours [27]. A rabbit anti-AIM2 primary antibody was from Bioss (Woburn, MA, USA); in previous studies (unpublished data) this AIM2 antibody showed similar staining patterns on cells and paraffin tissue sections when compared with other AIM2 antibodies from Abcam (Cambridge, UK) and Sigma/Atlas (Sigma-Aldrich, St Louis, MO, USA). The secondary antibodies were

TABLE 1 Subject demographics

	PBMCs		BAL cells
	Controls	PBB	
Subjects	20	20	35
Age years	2.2 (0.3–4.5)	1.6 (0.9–2.8)	2.6 (1.3–4.4)
Males	15 (75)	16 (80)	20 (57)
Culturable bacterial organisms n	N/A	3 (3–4)	3 (3–4)
Differential cell count $\times 10^6 \cdot L^{-1}$			
Total cell count	8.90 (8.18–10.20)	11.0 (9.05–12.2)	N/A
Neutrophils	2.88 (1.69–3.72)	3.63 (2.49–4.96)	N/A
Monocytes	0.80 (0.59–1.02)	1.09 (0.78–1.16)	N/A
Eosinophils	0.34 (0.12–0.67)	0.38 (0.19–0.59)	N/A
Lymphocytes	4.82 (3.81–5.87)	5.32 (4.04–6.60)	N/A
Immune cells %			
Neutrophils	N/A	N/A	23.0 (5.00–41.7)
Macrophages	N/A	N/A	65.0 (32.6–89.0)
Lymphocytes	N/A	N/A	7.60 (3.80–12.0)
Eosinophils	N/A	N/A	0.00 (0.00–0.30)

Data are presented as n, median (interquartile range) or n (%). PBMCs: peripheral blood mononuclear cells; BAL: bronchoalveolar lavage; PBB: protracted bacterial bronchitis; N/A: not applicable.

F(ab′)2 fragments of donkey serum IgG, AF488-conjugated antigoat, and AF594-conjugated antirabbit (both from Jackson Immunoresearch, West Grove, PA, USA). Confocal imaging and quantitative analysis of immunofluorescence using the ImageJ software (National Institutes of Health, Bethesda, MD, USA) were performed as previously described [25, 26]. Negative staining controls with cells incubated with secondary antibodies alone were included in each experiment. A "background" was defined as when the fluorescence did not exceed the brightness of negative control. To quantitate punctate immunofluorescence of NLRP3, AIM2 and cleaved IL-1β, the higher threshold of fluorescence intensity was set for the ImageJ software to count only bright particles, disregarding moderate homogenous fluorescence.

Enumeration of cell subsets and their cytokine response using flow cytometry

Frequency of monocytes, natural killer (NK) cells, T-cells and pro-IL-1β$^+$ cells were evaluated using intracellular cytokine staining. PBMC were stimulated with NTHi for 24 h and further incubated with Brefeldin A solution (BioLegend, San Diego, CA, USA) for 3.5 h. Cells were washed with fluorescence-activated cell sorter buffer (1% HI-FCS/PBS) blocked with normal goat IgG (Sigma-Aldrich) for 15 min on ice. The cells were then surface-stained with CD3-APC-Cy7, CD14-PerCP or CD56-AlexaFluor488 for 30 min on ice. After fixation and permeabilisation using Foxp3 Staining Buffer Set (eBioscience, San Diego, CA, USA), the cells were incubated further with intracellular cytokine IL-1β-AlexaFluor647 for 30 min at room temperature. The cells were then washed and fixed in 2%

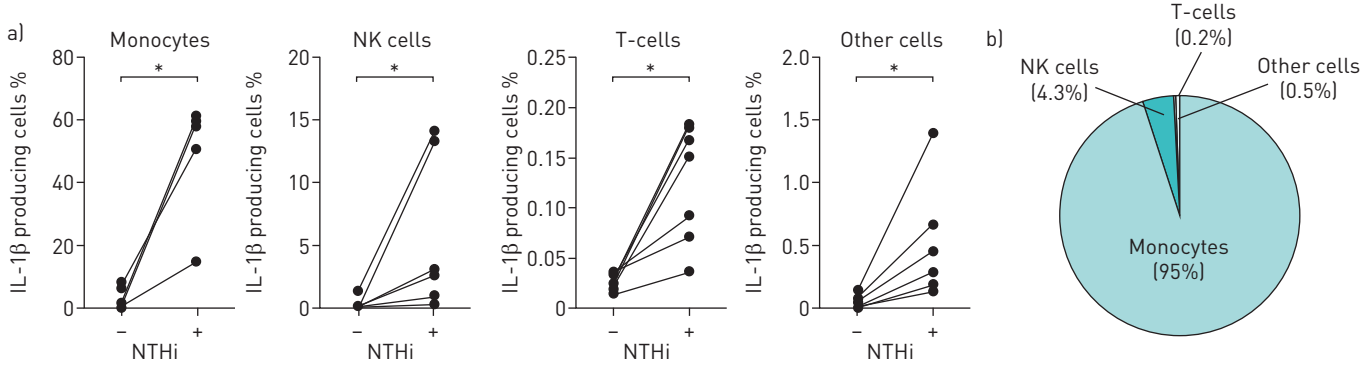

FIGURE 1 Interleukin (IL)-1β-producing cells in peripheral blood mononuclear cells (PBMCs). Gating strategy for flow cytometry: monocytes (CD14$^+$), NK cells (CD56$^+$) and T-cells (CD3$^+$) were obtained from total gated lymphocytes. Pro-IL-1β$^+$ cells were then evaluated in each of the cell subtypes. a) Frequency of pro-IL-1β$^+$ cells at 24 h post nontypeable *Haemophilus influenzae* (NTHi) stimulation (adult PBMCs, n=7). b) Percentage of each pro-IL-1β$^+$ cell type in total lymphocytes. *: p<0.05 by Wilcoxon matched-pairs signed rank test.

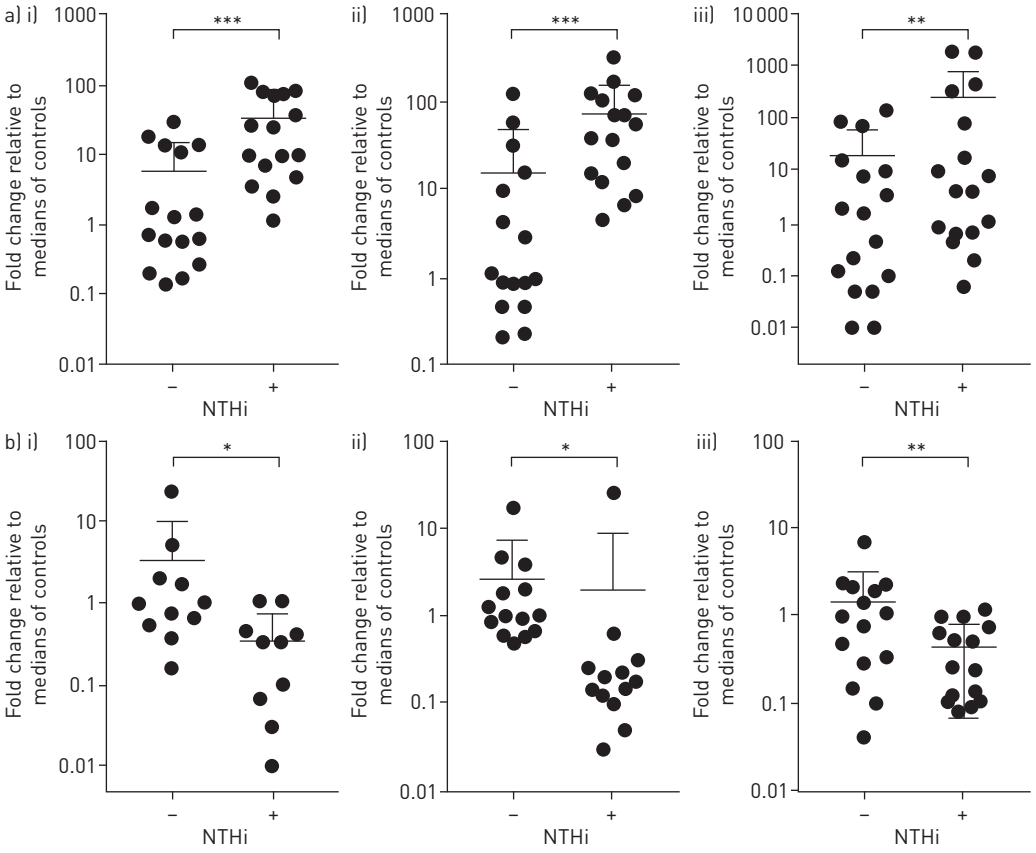

FIGURE 2 Expression of genes related to inflammasome activation in peripheral blood mononuclear cell (PBMC) and bronchoalveolar lavage (BAL) macrophages. PBMC or lung macrophages were cultured *ex vivo* for 24 h in the presence of nontypeable *Haemophilus influenzae* (NTHi). a) Expression of interleukin (*IL*)-*1β* in i) control PBMCs (n=16), ii) protracted bacterial bronchitis (PBB) PBMCs (n=16) and iii) BAL macrophages (n=18); b) expression of *NLRC4* in i) control PBMCs (n=11) ii) PBB PBMCs (n=14) and iii) BAL macrophages (n=15). Data are presented as individual data points, median and interquartile ranges. *: p<0.05; **: p<0.01; ***: p<0.001 by Wilcoxon matched-pairs signed rank test.

paraformaldehyde prior to analysis. A total of ~200 000 events were acquired using LSRFortessa X-20 (BD Biosciences). Data were analysed using the FlowJo Tree star software (version 7.6.1; Ashland, OR, USA). For intracellular cytokine staining, unstimulated background was subtracted from the data.

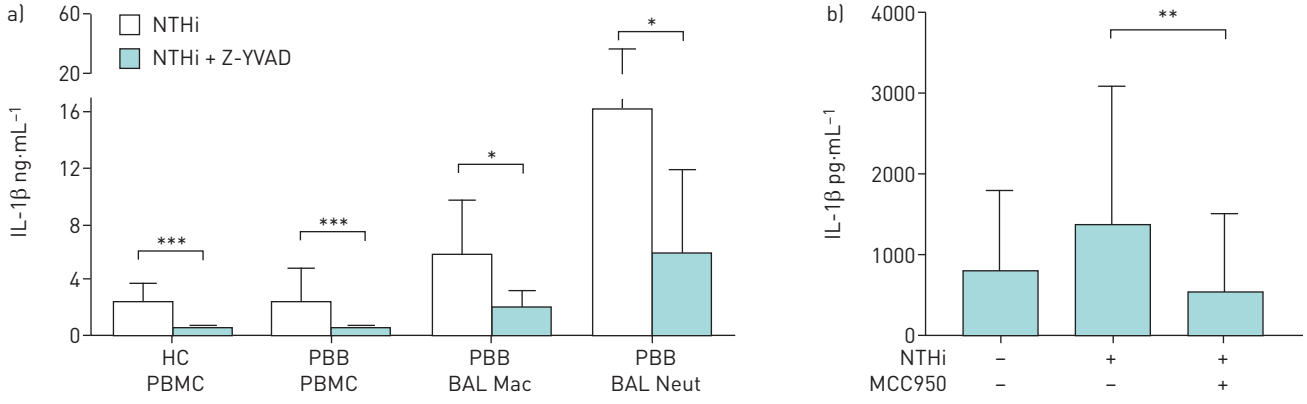

FIGURE 3 Effects of a caspase-1 inhibitor and NLRP3 inhibitor on nontypeable *Haemophilus influenzae* (NTHi)-induced interleukin (IL)-1β production. a) Peripheral blood mononuclear cells (PBMCs) and bronchoalveolar lavage (BAL) cells were cultured *ex vivo* for 24 h with NTHi in the presence or absence of the caspase-1 inhibitor (C1I) Z-YVAD-FMK. IL-1β produced by healthy control (HC) PBMCs (n=20), protracted bacterial bronchitis (PBB) PBMCs (n=20), BAL macrophages (PBB BAL Mac) (n=9) and BAL neutrophils (PBB BAL Neut) (n=9). b) BAL macrophages (n=9) were cultured *ex vivo* for 24 h in the presence of NTHi and NLRP3 inhibitor MCC950. Data are presented as mean±SD. *: p<0.05; **: p<0.01; ***: p<0.001 by Wilcoxon matched-pairs signed rank test.

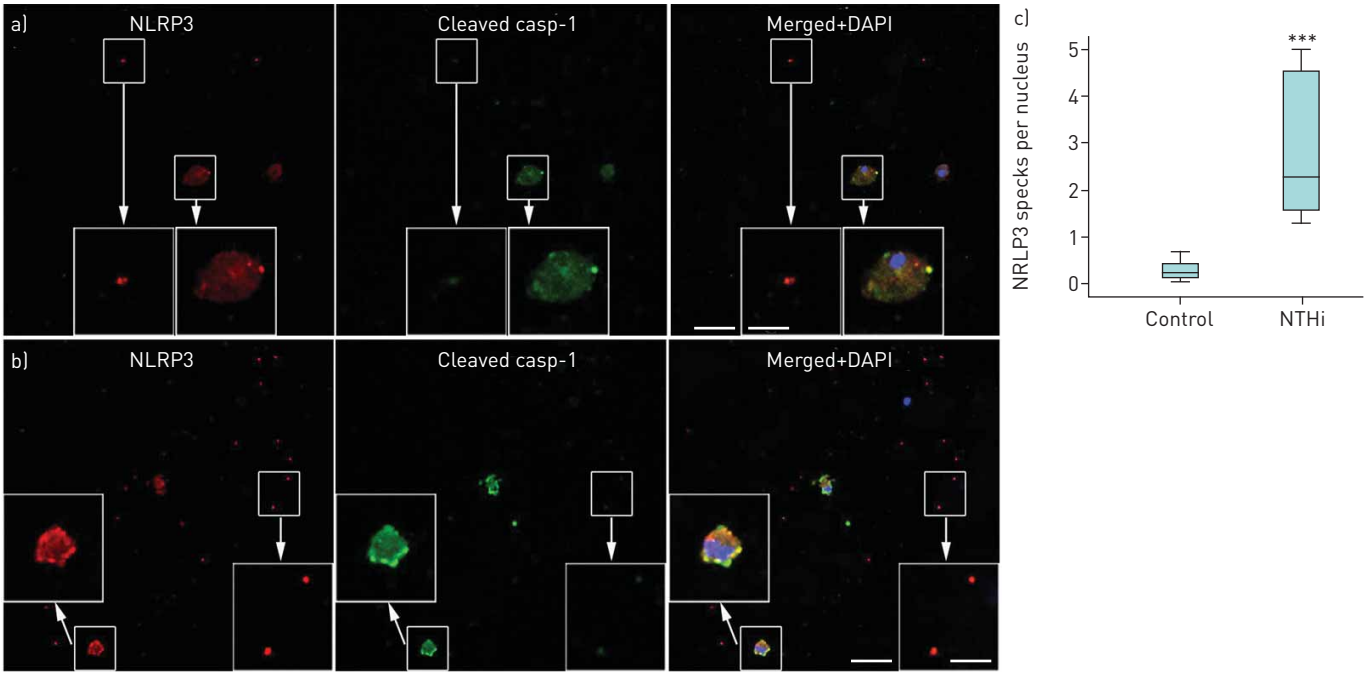

FIGURE 4 Visualisation of the NLRP3 inflammasome in bronchoalveolar lavage (BAL) macrophages. Representative confocal microphotos of cells cultured on chamberslides a) in control medium or b) stimulated with nontypeable *Haemophilus influenzae* (NTHi), both revealing specks of NLRP3 (red) and cleaved caspase-1 (green) in colocalisation (yellow/orange). Blue is the pseudocolour of DAPI (4′,6-diamidino-2-phenylindole). Scale bars=40 µm (main images) and 16 µm (inset images). c) Quantitative analysis of NLRP3 specks in control and NTHi-stimulated macrophages (n=8) showed a significant difference between the groups. ***: p<0.001 by Mann–Whitney U-test.

Outcome measures and data analysis

We applied the nonparametric Mann–Whitney U-tests to test the significance of differences between two study cohorts for analysis of gene expression, constitutive production of cytokines and quantitative immunofluorescence. For analysis of NTHi induction of cytokines and reduction of cytokine production by caspase-1 inhibitor, we used the Wilcoxon matched-pairs signed rank test. Statistical analyses were performed using PRISM software (version 6; GraphPad, San Diego, CA, USA), and two-tailed p-values <0.05 were considered significant.

Results

BAL cells were obtained from 35 children with PBB or bronchiectasis; PBMCs were obtained from 28 children with PBB and 20 healthy children (table 1). The age and sex distributions were similar between the study cohorts. Given our previous finding that NTHi can induce IL-1β production in PBMCs and BAL cells, our experiments focused on the mechanisms of IL-1β activation.

Pro-IL-1β$^+$ cells in PBMCs

In order to determine which cell subset expresses the most pro-IL-1β upon NTHi stimulation, we used intracellular staining and flow cytometry to enumerate the percentage of pro-IL-1β cells: monocytes (CD14$^+$ cells), NK cells (CD56$^+$ cells), T-cells (CD3$^+$ cells) and other cells. Very few unstimulated cells produced IL-1β (adult PBMCs, n=7; figure 1a). NTHi stimulation increased the frequency of pro-IL-1β cells including monocytes, NK cells and T-cells (p<0.05 for all). The majority of pro-IL-1β cells in NTHi-stimulated PBMCs are monocytes (95%), NK cells (4.3%) and T-cells (0.2%) (figure 1b).

Inflammasome-related gene transcription

To test the regulation of different inflammasome complexes after NTHi stimulation, PBMCs from five healthy donors were infected with NTHi *in vitro*, and gene expression was measured. NTHi stimulation led to upregulation of *IL-1β* (p<0.01) and downregulation of *NLRC4* (p<0.01) (online supplementary figure S1). There were trends for enhanced *NLRP3* and *AIM2* expression in NTHi-stimulated cells; however, NTHi had no discernible effect on *NLRP1* and *NLRP6* expression. These findings were further validated in a larger cohort. Stimulation with NTHi *in vitro* induced significant upregulation of *IL-1β* in PBMCs from participants with PBB (47-fold, p<0.001), age-matched healthy controls (17-fold, p<0.001)

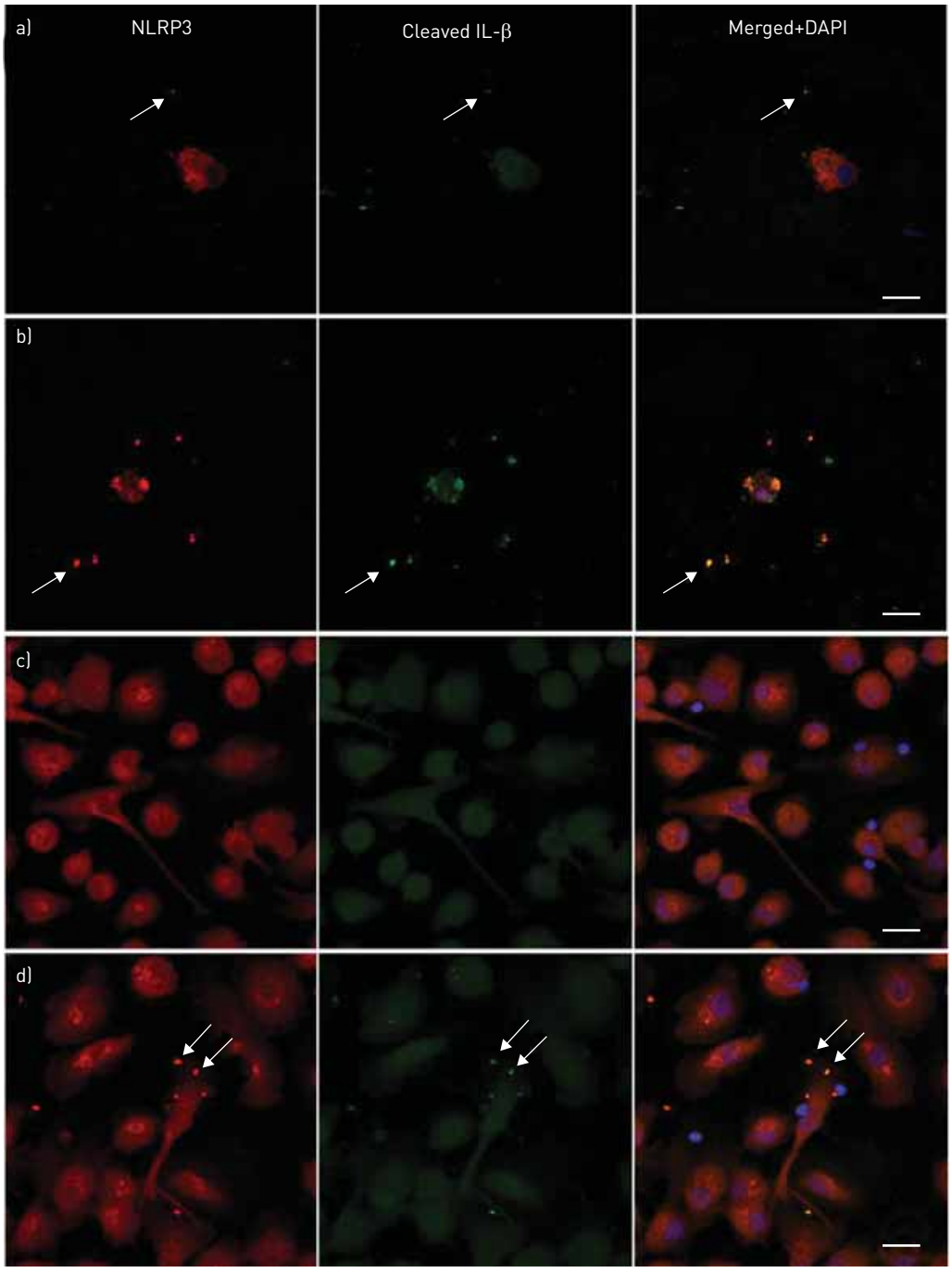

FIGURE 5 Colocalisation of NLRP3 specks with cleaved interleukin (IL)-1β in bronchoalveolar lavage (BAL) macrophages, and nontypeable *Haemophilus influenzae* (NTHi)-stimulated monocyte-derived macrophages. BAL macrophages cultured for 24 h in a) control medium or b) in presence of NTHi both revealed specks of NLRP3 (red) and cleaved IL-1β (green) in colocalisation (yellow/orange; arrows). Monocyte-derived macrophages showed c) only homogenous fluorescence when cultured in control medium, but d) revealed numerous NLRP3/cleaved IL-1β specks (arrows) when stimulated with NTHi. Blue is the pseudocolour of DAPI (4',6-diamidino-2-phenylindole). Scale bars=20 µm. Images are representative confocal microphotos of cells from at least four donors.

and BAL macrophages from patients with PBB (four-fold, $p<0.01$) (figure 2a). In addition, NTHi stimulation downregulated expression of *NLRC4* in PBMC from participants with PBB (six-fold, $p<0.05$), age-matched healthy controls (three-fold, $p<0.05$) and BAL macrophages from patients with PBB (four-fold, $p<0.01$) (figure 2b). Thus, these mechanisms appear to be common across a variety of cell types.

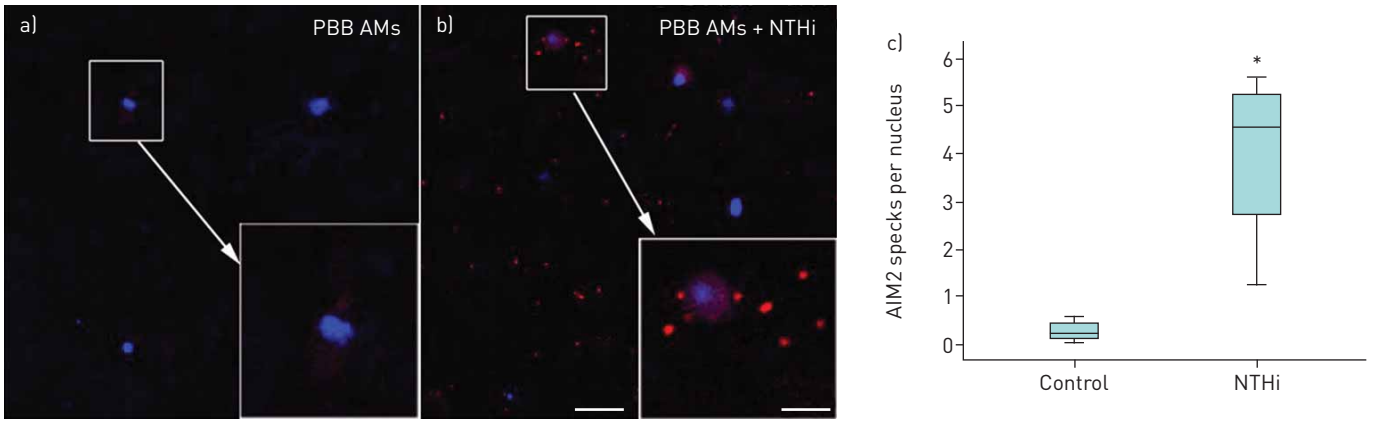

FIGURE 6 Nontypeable *Haemophilus influenzae* (NTHi)-induced increased specks of AIM2 in bronchoalveolar lavage (BAL) macrophages. Representative confocal images of AIM2 (red) in chamberslides of BAL macrophages cultured for 24 h in a) control medium or b) in presence of NTHi. Blue is the pseudocolour of DAPI (4′,6-diamidino-2-phenylindole). Scale bars=40 µm (main images) and 16 µm (inset images). c) Quantitative analysis of AIM2 specks in control and NTHi-stimulated samples (n=4) showed a significant difference between the groups. *: p<0.05 by Mann–Whitney U-test.

Effects of caspase-1 and NLRP3 selective inhibition

To test the dependence of NTHi-induced IL-1β secretion on inflammasome(s), we pre-exposed cells to Z-YVAD-FMK, a caspase-1 selective inhibitor, and MCC950, a selective NLRP3 inhibitor, before NTHi stimulation. Both inhibitors significantly reduced NTHi-induced IL-1β secretion by PBMC and BAL macrophages. In NTHi-stimulated cells, IL-1β production was largely dependent on caspase-1 (83% average inhibition in 20 healthy PBMCs, 69% inhibition in 20 PBB PBMCs and 25% inhibition in nine BAL macrophages; p<0.001, p<0.001 and p<0.05, respectively; figure 3a) and NLRP3 (58% inhibition in nine BAL macrophages, p<0.01; figure 3b).

Quantitative immunofluorescence of NLRP3 and AIM2

For demonstration of NLRP3 inflammasome activation, cell preparations in chamber slides and cytospins were dually labelled for NLRP3 and cleaved caspase-1, followed by analysis using confocal microscopy. BAL macrophages cultured in the absence or presence of NTHi (24 h) revealed NLRP3 punctate immunofluorescence colocalised with cleaved caspase-1 (figure 4a and b). The amount of such punctate immunofluorescence was significantly increased by NTHi stimulation (figure 4c). There were similar colocalied immunofluorescence of NLRP3/cleaved IL-1β in BAL macrophages (figure 5a and b). Monocyte-derived macrophages from subjects with PBB and healthy controls showed only homogenous fluorescence when cultured in control medium (figure 5c), while NTHi-stimulated cells produced numerous NLRP3/cleaved IL-β punctate immunofluorescence (figure 5d). In BAL macrophages, a significant increase in AIM2 punctate immunofluorescence following stimulation with NTHi was shown (figure 6). In keeping with the NTHi-induced caspase-1-dependent secretion of IL-1β from PBMCs (figure 3), we detected punctate immunofluorescence of NLRP3 and AIM2 in both NTHi-stimulated PBMCs (figure 7a and b) and blood monocytes (figure 7c and d). In addition, colocalisation of AIM2 punctate immunofluorescence with cleaved IL-1β was demonstrated (figure 7d).

Discussion

The inflammatory mechanisms involved in PBB are poorly understood. Of the many protective inflammatory pathways induced by infectious agents, pleiotropic cytokines of the IL-1 family stand out as central mediators of innate immunity and inflammation. We have previously reported that NTHi induces IL-1β production by PBMC and lung macrophages from PBB and healthy individuals [28], and airway concentrations of IL-1β are associated with cough severity in PBB [12]. To prevent excessive and detrimental inflammation, the effects of these potent cytokines are tightly controlled in multiple steps, inflammasomes being one of the key regulators [29]. The role of NLRP3 has been studied in other inflammatory diseases such as asthma [30, 31] and chronic obstructive pulmonary disease (COPD) [13], but to our knowledge, this study is the first to address the role of IL-1β and inflammasome activation in children with PBB. This study sought to examine IL-1β regulation in PBB. Our key findings are as follows. Firstly, NTHi-induced IL-1β production is largely caspase-1- and NLRP3-dependent in both PBMCs and lung macrophages from children with PBB. Secondly, reduced expression of *NLRC4* and co-activation of NLRP3 and AIM2 may be important in airway IL-1β activation.

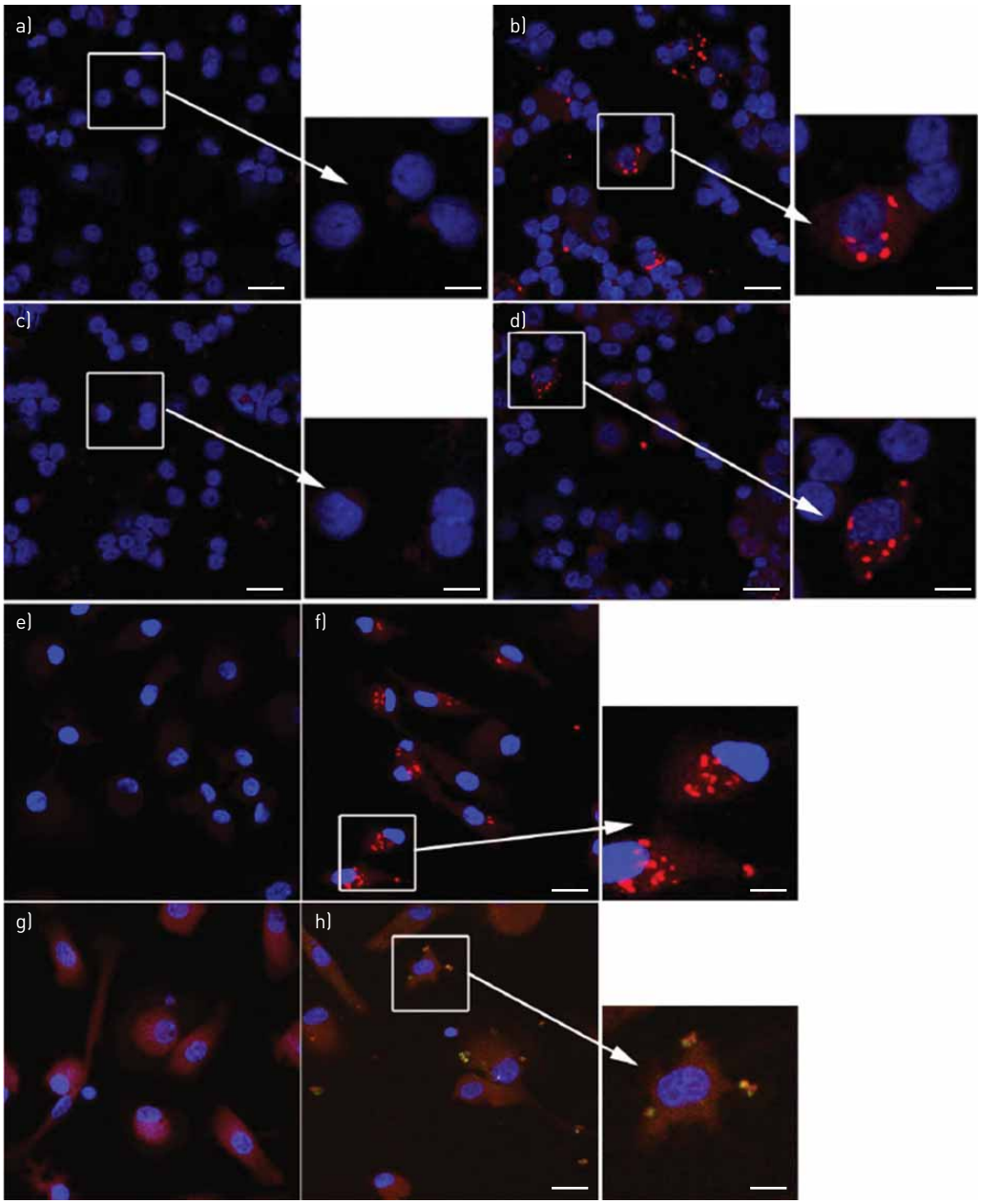

FIGURE 7 Nontypeable *Haemophilus influenzae* (NTHi)-induced inflammasome specks in peripheral blood mononuclear cell (PBMC) and blood monocytes. Specks of NLRP3 (red) were not detected in a) PBMCs cultured in control medium, but were readily detected in b) the presence of NTHi. Specks of AIM2 (red) were not detected in PBMCs c) cultured in control medium, but were readily detected in d) the presence of NTHi. Specks of NLRP3 (red) were e) not detected in monocytes cultured in control medium, but f) were readily detected in the presence of NTHi. g) and h) Dual labelling of NTHi-stimulated monocytes revealed colocalised specks of AIM2 (red) and cleaved interleukin (IL)-1β (green). Yellow is merged colour of red and green. Blue is the pseudocolour of DAPI (4′,6-diamidino-2-phenylindole). Scale bars=20 µm (main images) and 8 µm (inset images). Images are representative confocal microphotos of cells from of at least four donors.

Analysis of gene expression and spontaneous production of IL-1β in PBMCs revealed no difference between children with PBB and controls, indicating that the inflammation in PBB was not systemic, but limited to the airway. Whereas only low amounts of secreted IL-1β were detected in PBMCs from PBB patients (0–1 pg·mL^{-1}), IL-1β was readily detected (2000–7000 pg·mL^{-1}) in BAL-derived macrophages. Consistent with this, confocal immunofluorescence analysis of PBB BAL macrophages revealed specks of NLRP3 colocalised with cleaved caspase-1 and cleaved IL-1β, indicating NLRP3 inflammasome activation. Although no age-matched healthy control BAL macrophages were available for comparison (it is very difficult to obtain BAL macrophages from healthy children due to ethical sampling difficulties), similar

speckle immunofluorescence was very rarely, if never, observed in our cultures of unstimulated monocyte-derived macrophages or PBMCs.

We applied a model of inflammasome activation by NTHi, a micro-organism commonly associated with PBB. NTHi-induced NLRP3 inflammasome activation *ex vivo* in the context of COPD has been reported previously, evidenced by an increase of caspase-1-dependent IL-1β secretion and increased protein expression of NLRP3 and caspase-1 [13]. In keeping with the cited study, we found that *IL-1β* gene expression in human PBMC responded significantly and positively to stimulation with NTHi. An increased IL-1β-mediated inflammation in PBB would be expected from the previously reported upregulation of TLR2/4 [10], ligation of which is generally believed to upregulate expression of *IL-1β* among other pro-inflammatory genes *via* the MyD88-NF-kB axis [32]. In parallel with *IL-1β* gene upregulation, NTHi stimulation also induced maturation of the cytokine protein, evidenced by increased IL-1β secretion, and specks of cleaved IL-1β associated with NLRP3/AIM2. Importantly, both the caspase-1 inhibitor Z-YVAD, and the NLRP3 inhibitor MCC950 significantly reduced NTHi-induced secretion of IL-1β, supporting a role for inflammasome activation.

Our data suggest that NTHi invasion of the cell may cause complex changes in inflammasome pathways. In contrast to the activation of NLRP3 and AIM2, *NLRC4* gene transcription in NTHi-stimulated PBMCs and BAL macrophages was significantly downregulated. We did not investigate NLRC4 protein expression, but given that the NLRC4 inflammasome is implicated in protection from flagellated bacteria such as *Salmonella* and *Burkholderia* [33], and that flagellar expression may exist in some clinical isolates of NTHi [34], the downregulated gene expression warrants further investigation to test the possibility that NTHi may also utilise NLRC4 inhibition as a means to escape host immunity.

Caspase-1 is required for IL-1β production by monocyte and alveolar macrophages [35, 36]. Others have reported that the molecular pathways regulating inflammasome activation differ between monocytes and macrophages [37]. If BAL macrophages are indeed in a "tolerant" state in PBB, this might impact on the extent to which caspase-1 is able to regulate IL-1β production. Downregulation of cytokine production is a feature of Gram-negative sepsis and endotoxaemia, and there is strong evidence linking reduced IL-1β secretion in sepsis to reduced pro-caspase-1 and cleaved caspase-1 protein [38].

In conclusion, this study supports the hypothesis that the NLRP3 inflammasome may be the major detector of early NTHi intrusion, and that the AIM2 inflammasome, which specifically detects double-stranded DNA in the cytosolic compartment may become more important in later stages when the pathogen escapes the endosomal compartment. Taken together, our data suggest that co-activation of the NLRP3 and AIM2 inflammasomes plays a role in IL-1β induction, and that airway invasion with potential pathogens such as NTHi may be a potential mechanism for negating protective mechanisms in PBB and other chronic respiratory diseases.

Acknowledgements

We thank all the children and their parents who participated in this study. We also thank Christopher Bourke and Nitin Kapur (Lady Cilento Children's Hospital, Brisbane, Australia) for allowing us to recruit their patients into the study; Judith Zenchyson (Children's Centre for Health Research, Queensland University of Technology, Brisbane) for sample collection; and Victoria Timbrell and Liisa Murray (Diamantina Institute, The University of Queensland, Brisbane) for their assistance with processing the specimens.

Author contributions: A.C-H. Chen, H.B. Tran, K.J. Baines, A.A.B. Robertson, M. Carroll, K. Schroder, J.L. Simpson, P.G. Gibson, G. Hodge, I.B. Masters, H.M. Buntain, A.B. Chang, S. Hodge and J.W. Upham conceived and designed the study; A.C-H. Chen, H.B. Tran, Y. Xi, S.T. Yerkovitch, S.J. Pizzutto, M.A. Cooper, H.L. Petsky and S.J. Prime acquired the data; A.C-H. Chen, H.B. Tran, Y. Xi, S.T. Yerkovitch, A.B. Chang, S. Hodge and J.W. Upham analysed and interpreted the data; A.C-H. Chen, H.B. Tran, Y. Xi, S.T. Yerkovitch, H.L. Petsky, A.B. Chang, S. Hodge and J.W. Upham drafted the manuscript for important intellectual content; and the final version to be published was approved by all authors.

References

1 Marchant JM, Masters IB, Taylor SM, *et al.* Evaluation and outcome of young children with chronic cough. *Chest* 2006; 129: 1132–1141.
2 McShane PJ, Naureckas ET, Tino G, *et al.* Non-cystic fibrosis bronchiectasis. *Am J Respir Crit Care Med* 2013; 188: 647–656.
3 Chang AB, Redding GJ, Everard ML. Chronic wet cough: protracted bronchitis, chronic suppurative lung disease and bronchiectasis. *Pediatr Pulmonol* 2008; 43: 519–531.
4 Chang AB, Upham JW, Masters IB, *et al.* Protracted bacterial bronchitis: the last decade and the road ahead. *Pediatr Pulmonol* 2016; 51: 225–242.
5 Kompare M, Weinberger M. Protracted bacterial bronchitis in young children: association with airway malacia. *J Pediatr* 2012; 160: 88–92.

6 Kapur N, Grimwood K, Masters IB, *et al.* Lower airway microbiology and cellularity in children with newly diagnosed non-CF bronchiectasis. *Pediatr Pulmonol* 2012; 47: 300–307.
7 Narang R, Bakewell K, Peach J, *et al.* Bacterial distribution in the lungs of children with protracted bacterial bronchitis. *PLoS One* 2014; 9: e108523.
8 Wurzel DF, Marchant JM, Yerkovich ST, *et al.* Protracted bacterial bronchitis in children: natural history and risk factors for bronchiectasis. *Chest* 2016; 150: 1101–1108.
9 Erwin AL, Smith AL. Nontypeable *Haemophilus influenzae*: understanding virulence and commensal behavior. *Trends Microbiol* 2007; 15: 355–362.
10 Marchant JM, Gibson PG, Grissell TV, *et al.* Prospective assessment of protracted bacterial bronchitis: airway inflammation and innate immune activation. *Pediatr Pulmonol* 2008; 43: 1092–1099.
11 Chang AB, Yerkovich ST, Gibson PG, *et al.* Pulmonary innate immunity in children with protracted bacterial bronchitis. *J Pediatr* 2012; 161: 621–625.
12 Baines KJ, Upham JW, Yerkovich ST, *et al.* Mediators of neutrophil function in children with protracted bacterial bronchitis. *Chest* 2014; 146: 1013–1020.
13 Rotta Detto Loria J, Rohmann K, Droemann D, *et al.* Nontypeable *Haemophilus influenzae* infection upregulates the NLRP3 inflammasome and leads to caspase-1-dependent secretion of interleukin-1β – a possible pathway of exacerbations in COPD. *PLoS One* 2013; 8: e66818.
14 Rogers GB, Zain NM, Bruce KD, *et al.* A novel microbiota stratification system predicts future exacerbations in bronchiectasis. *Ann Am Thorac Soc* 2014; 11: 496–503.
15 Chen AC, Martin ML, Lourie R, *et al.* Adult non-cystic fibrosis bronchiectasis is characterised by airway luminal Th17 pathway activation. *PLoS One* 2015; 10: e0119325.
16 Hodge S, Upham JW, Pizzutto S, *et al.* Is alveolar macrophage phagocytic dysfunction in children with protracted bacterial bronchitis a forerunner to bronchiectasis? *Chest* 2016; 149: 508–515.
17 Brusselle GG, Provoost S, Bracke KR, *et al.* Inflammasomes in respiratory disease: from bench to bedside. *Chest* 2014; 145: 1121–1133.
18 Pinkerton JW, Kim RY, Robertson AAB, *et al.* Inflammasomes in the lung. *Mol Immunol* 2017; 86: 44–55.
19 Kapur N, Masel JP, Watson D, *et al.* Bronchoarterial ratio on high-resolution CT scan of the chest in children without pulmonary pathology: need to redefine bronchial dilatation. *Chest* 2011; 139: 1445–1450.
20 Chang AB, Newman RG, Carlin JB, *et al.* Subjective scoring of cough in children: parent-completed *vs* child-completed diary cards *vs* an objective method. *Eur Respir J* 1998; 11: 462–466.
21 de Blic J, Midulla F, Barbato A, *et al.* Bronchoalveolar lavage in children. ERS Task Force on bronchoalveolar lavage in children. *Eur Respir J* 2000; 15: 217–231.
22 Wurzel DF, Marchant JM, Clark JE, *et al.* Wet cough in children: infective and inflammatory characteristics in broncho-alveolar lavage fluid. *Pediatr Pulmonol* 2014; 49: 561–568.
23 Hodge S, Hodge G, Scicchitano R, *et al.* Alveolar macrophages from subjects with chronic obstructive pulmonary disease are deficient in their ability to phagocytose apoptotic airway epithelial cells. *Immunol Cell Biol* 2003; 81: 289–296.
24 Pizzutto SJ, Yerkovich ST, Upham JW, *et al.* Children with chronic suppurative lung disease have a reduced capacity to synthesize interferon-gamma *in vitro* in response to non-typeable *Haemophilus influenzae*. *PLoS One* 2014; 9: e104236.
25 Tran HB, Barnawi J, Ween M, *et al.* Cigarette smoke inhibits efferocytosis *via* deregulation of sphingosine kinase signaling: reversal with exogenous S1P and the S1P analogue FTY720. *J Leukoc Biol* 2016; 100: 195–202.
26 Hodge S, Tran HB, Hamon R, *et al.* Nonantibiotic macrolides restore airway macrophage phagocytic function with potential anti-inflammatory effects in chronic lung diseases. *Am J Physiol Lung Cell Mol Physiol* 2017; 312: L678–L687.
27 Tran HB, Lewis MD, Tan LW, *et al.* Immunolocalization of NLRP3 inflammasome in normal murine airway epithelium and changes following induction of ovalbumin-induced airway inflammation. *J Allergy* 2012; 2012: 819176.
28 Chen AC, Xi Y, Carroll M, *et al.* Cytokine responses to two common respiratory pathogens in children are dependent on interleukin-1β. *ERJ Open Res* 2017; 3: 000025-2017.
29 Garlanda C, Dinarello CA, Mantovani A. The interleukin-1 family: back to the future. *Immunity* 2013; 39: 1003–1018.
30 Kim RY, Pinkerton JW, Essilfie AT, *et al.* Role for NLRP3 inflammasome-mediated, IL-1β-dependent responses in severe, steroid-resistant asthma. *Am J Respir Crit Care Med* 2017; 196: 283–297.
31 Simpson JL, Phipps S, Baines KJ, *et al.* Elevated expression of the NLRP3 inflammasome in neutrophilic asthma. *Eur Respir J* 2014; 43: 1067–1076.
32 Takeda K, Akira S. Toll receptors and pathogen resistance. *Cell Microbiol* 2003; 5: 143–153.
33 Zhao Y, Yang J, Shi J, *et al.* The NLRC4 inflammasome receptors for bacterial flagellin and type III secretion apparatus. *Nature* 2011; 477: 596–600.
34 Carabarin-Lima A, Lozano-Zarain P, Castaneda-Lucio M, *et al.* Flagellar expression in clinical isolates of non-typeable *Haemophilus influenzae*. *J Med Microbiol* 2017; 66: 592–600.
35 Wu J, Yan Z, Schwartz DE, *et al.* Activation of NLRP3 inflammasome in alveolar macrophages contributes to mechanical stretch-induced lung inflammation and injury. *J Immunol* 2013; 190: 3590–3599.
36 Shimada K, Crother TR, Karlin J, *et al.* Caspase-1 dependent IL-1β secretion is critical for host defense in a mouse model of *Chlamydia pneumoniae* lung infection. *PLoS One* 2011; 6: e21477.
37 Netea MG, Nold-Petry CA, Nold MF, *et al.* Differential requirement for the activation of the inflammasome for processing and release of IL-1β in monocytes and macrophages. *Blood* 2009; 113: 2324–2335.
38 Giamarellos-Bourboulis EJ, van de Veerdonk FL, Mouktaroudi M, *et al.* Inhibition of caspase-1 activation in Gram-negative sepsis and experimental endotoxemia. *Crit Care* 2011; 15: R27.